JOURNAL OF SOLID STATE CHEMISTRY 49, 1–5 (1983)

Preparation, Crystallization, and Magnetic Properties of Amorphous $Fe_{100-x}B_x$ ($18 \leq x \leq 42$)

F. KANAMARU, S. MIYAZAKI, M. SHIMADA, AND M. KOIZUMI

Institute of Scientific and Industrial Research, Osaka University, Mihogaoka, Ibaraki, Osaka 567, Japan

K. ODA

Research Institute for Non-crystalline Materials, School of Engineering, Okayama University, Tsushima, Okayama 700, Japan

AND Y. MIMURA

Central Laboratory of KDD, Nakameguro, Meguro-ku, Tokyo 153, Japan

Received October 11, 1982; in revised form February 18, 1983

Amorphous $Fe_{100-x}B_x$ alloys were prepared by the rf-sputtering method in a chemical composition range of $18 \leq x \leq 42$. The crystallization temperature of the amorphous alloys increases with the B contents up to near $x = 36$, above which the crystallization temperature decreases monotonically. This anomaly is reflected in the composition dependence of the Curie temperature and of the coercive force of the amorphous alloys.

A large number of measurements on physical properties as well as on the structure of amorphous Fe–B alloys have been made in the last few years (*1–4*). It is well known that the physical properties of such amorphous alloys strongly depend on the B content (*5–9*). These studies have been limited to the narrow composition range of $11 \leq x \leq 25$, because most of the amorphous alloys were prepared by rapid quenching from the melt, with composition ranges for the eutectic composition near 20 at.% B. For further understanding of the properties of the amorphous Fe–B alloys as a function of B content, a few studies have been done on vapor-deposition films with higher boron content (*10–14*).

In this work, a co-sputtering method was applied for preparation of the amorphous $Fe_{100-x}B_x$ alloys. A crystallochemical characterization of the vapor-deposited $Fe_{100-x}B_x$ ($13 \leq x \leq 42$), as well as the composition dependence of the crystallization temperature, the Curie temperature, and the coercive force of the alloys, is described in this paper.

The rf-sputtering apparatus used for preparation of amorphous $Fe_{100-x}B_x$ alloys was a ULVAC-SBR-1104 unit. A target was placed on the lower electrode and a substrate was attached to the center of the upper electrode. The targets used for co-sputtering are composed of an Fe disk (100 mm ϕ), geometrically arranged B disks

0022-4596/83 $3.00

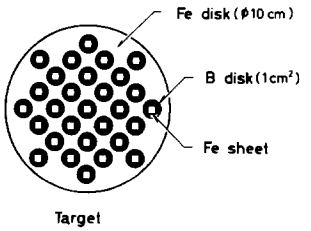

FIG. 1. Typical assembly of the target for co-sputtering.

(11.3 mm ϕ), and small square Fe foils (3 × 3 to 8 × 8 mm^2) as shown in Fig. 1. The B area coverage on the target was adjusted to a desired value by changes in both the number of the B disks (33–43) and in the dimension of the square Fe foil. The square Fe foils were used for control of the B area coverage on targets with low B area coverage. Both a slide glass and a polyimide film were used as the substrate. Rf-sputtering was carried out by using Ar gas as a sputtering gas.

Crystallochemical Characterization

The chemical composition of the vapor-deposited alloys was determined by atomic absorption spectroscopy. As shown in Fig. 2, it is confirmed that the average chemical composition of the alloys is in proportion to the area coverage of B on the targets, even though the atomic ratio of B to Fe in the alloys is lower than the area ratio of B to Fe on the targets.

The homogeneity of the composition in each alloy was checked using an electron probe microanalyzer. The result showed that the alloys prepared by co-sputtering have a uniform distribution of B and Fe, despite the use of the heterogeneous composite target.

The alloy of 13 at.% B exhibits X-ray diffraction lines which are attributed to an α-type Fe crystalline phase (perhaps B-containing α-Fe), while the alloys of 18 to 42 at.% B exhibit broad halo patterns. The electron diffraction patterns taken on the latter samples also exhibit only halo patterns, indicating that the alloys of 18 to 42 at.% B produced by rf-sputtering are amorphous.

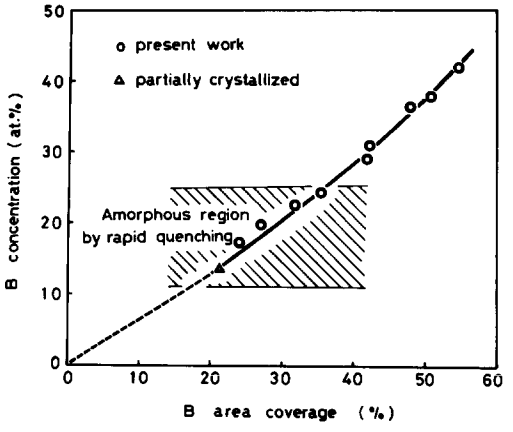

FIG. 2. Chemical composition of the sputter-deposited $Fe_{100-x}B_x$ alloys vs B area coverage on target.

Crystallization of the Amorphous $Fe_{100-x}B_x$ Alloys

The crystallization process of the amorphous alloys was examined by both DTA and X-ray diffraction methods. The results are listed in Table I.

The manner in which amorphous alloys of less than 25 at.% B crystallized on heat-

TABLE I

HEAT TREATMENT CONDITIONS AND PRECIPITATED CRYSTAL PHASES

Composition	As-sputtered film	Temperature (°C)	Crystal phases
$Fe_{82}B_{18}$	Amorphous	460	α-Fe, Fe_3B
$Fe_{80}B_{20}$	Amorphous	460	α-Fe, Fe_3B
$Fe_{77}B_{23}$	Amorphous	440	α-Fe, Fe_3B
		460	α-Fe, Fe_2B
$Fe_{71}B_{29}$	Amorphous	480	α-Fe, Fe_2B
$Fe_{62}B_{38}$	Amorphous	460	FeB, Fe_2B, α-Fe
$Fe_{58}B_{42}$	Amorphous	410	FeB
		460	FeB, Fe_2B, α-Fe

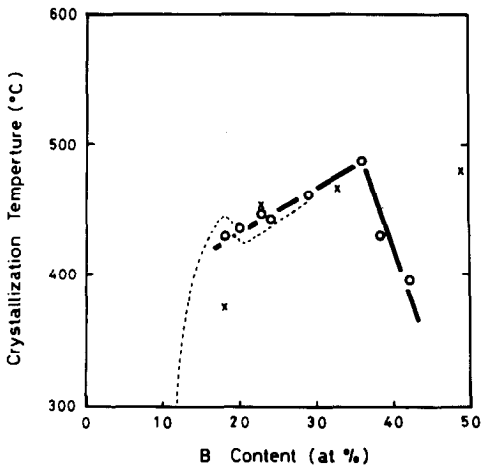

FIG. 3. Crystallization temperature vs B content for the amorphous $Fe_{100-x}B_x$ alloys at 10 deg/min compared to some typical works published previously. ○ present work; --- (Ref. (*5*)); × (Ref. (*11*)).

ing was almost the same as that reported in the literature (*10, 16–18*), e.g., Fe_3B and α-Fe deposited in the temperature range from 400 to 500°C. No Fe_3B crystallized from the amorphous alloys of more than 29 at.% B in the same temperature range. Fe_2B and α-Fe crystallized from the amorphous alloys of 29 to 36 at.% B. On annealing the amorphous alloys of 38 and 42 at.% B, FeB (B–B distance; 0.177 nm (*19*)) deposited in the amorphous matrix; the crystallization of Fe_2B and α-Fe occurred on further annealing at higher temperature.

(42 at.% B)

$$\text{amorphous} \xrightarrow{398°C} \text{FeB} + \text{"amorphous"} \xrightarrow{460°C} \text{Fe}_2\text{B} + \alpha\text{-Fe}$$

It has been demonstrated that some noncrystalline alloys have local atomic arrangements similar to their crystalline counterparts (*20, 21*). If this concept is applied to the present amorphous alloys, it is expected that the first-deposited crystalline phase reflects the local short-range order of the amorphous state.

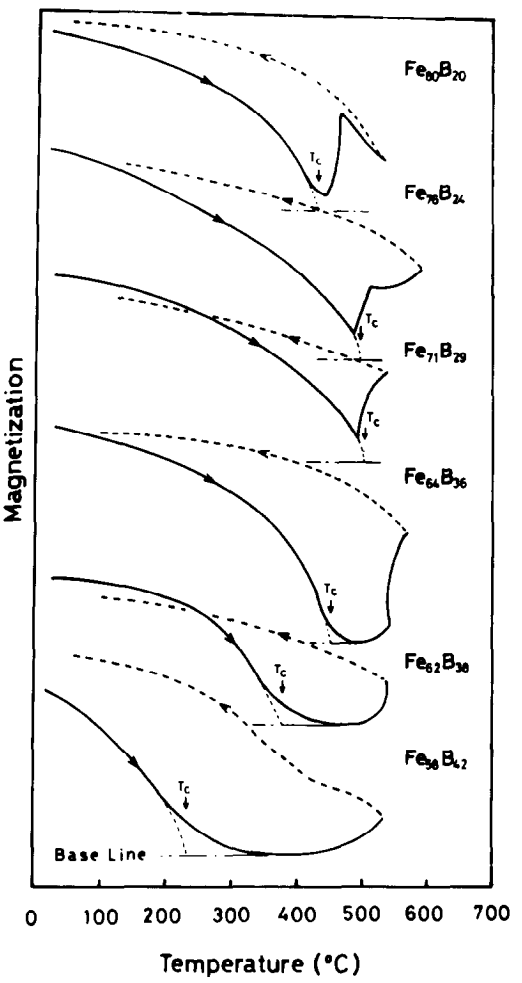

FIG. 4. Temperature dependence of the magnetization at 5 kOe for the amorphous $Fe_{100-x}B_x$ alloys.

The crystallization temperature (T_{cryst}) of the amorphous alloys, determined from the first exothermic peak in DTA curve (10 deg/min), is plotted as a function of B content in Fig. 3. T_{cryst} increases with increase in the amount of B in the composition range from 18 to 36 at.% B, while T_{cryst} decreases with increase in B in the composition range of x larger than 36.

Magnetic Properties

Figure 4 shows the temperature dependence of the magnetization at 5 kOe. The

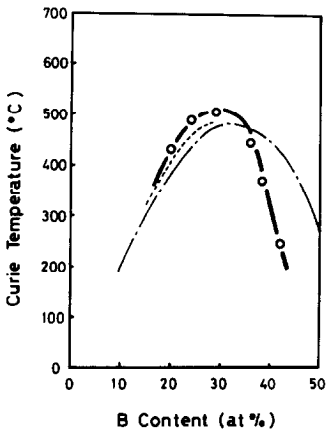

FIG. 5. Curie temperature vs B content for the amorphous $Fe_{100-x}B_x$ alloys. O present work; --- (Ref. (*22*)); ·-·- (Ref. (*15*)).

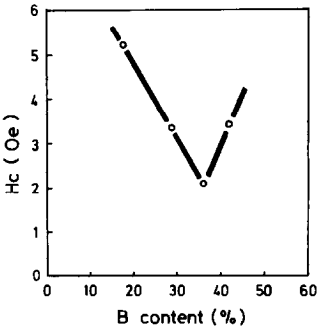

FIG. 6. Coercive force (H_c) vs B content for the amorphous $Fe_{100-x}B_x$ alloys deposited onto a slide-glass substrate.

as-deposited amorphous alloys on a polyimide film were subjected to the magnetic measurement without separating the amorphous alloys from the substrate. Therefore, the values of magnetization in Fig. 4 (unit of longitudinal axis) are represented on an arbitrary scale. As seen in Fig. 4, the magnetization for the amorphous alloys of less than 29 at.% B decreases gradually with rising temperature up to 400–500°C, and then increases rapidly at the crystallization temperature before the magnetization vanishes. The Curie temperature (T_c) of the amorphous alloys was determined from the σ^2 vs T curve over the temperature. On the other hand, the magnetization of the amorphous alloys of 36, 38, and 42 at.% B vanishes at the T_c of the amorphous alloys and then increases rapidly at a higher temperature corresponding to the crystallization process as described above. Figure 5 shows the composition dependence of T_c of the amorphous alloys. T_c increases with increasing B content up to about 33 at.% B, and decreases with B content in the composition range beyond 36 at.% B.

The coercive force (H_c) of the amorphous alloys was determined from the magnetization-applied magnetic field loops obtained at room temperature by a vibrating sample magnetometer. The measurement was carried out on the as-deposited amorphous alloys on a slide-glass substrate without annealing them, because of the difficulty of removing the amorphous alloys from the substrate. Therefore, the H_c values obtained in this work are larger than the reported ones for the annealed amorphous alloys with the same composition (*21, 23*). The composition dependence of H_c is shown in Fig. 6. In the range of less than 36 at.% B, H_c decreases with increase of the B concentration, while it increases with the B content for the higher B compositions.

References

1. N. S. KAZAMA, M. MITERA, AND T. MASUMOTO, "Rapidly Quenched Metals III" (B. Cantor, Ed.), Vol. 2, p. 164, The Metal Society (1978).
2. T. EGAMI AND S. D. DAHLGREN, *J. Appl. Phys.* **49**, 1703 (1978).
3. R. OSHIMA AND F. E. FUJITA, *Japan J. Appl. Phys.* **20**, 1 (1981).
4. Y. WASED AND H. S. CHEN, *Phys. Status Solidi A* **49**, 387 (1978).
5. F. E. LUBORSKY, H. H. LIEBERMANN, J. J. BECKER, AND J. L. WALTER, "Rapidly Quenched Metals III" (B. Cantor, Ed.), Vol. 2, p. 188, The Metal Society (1978).
6. M. TAKAHASHI, M. KOSHIMURA, AND T. ABUZUKA, *Japan J. Appl. Phys.* **20**, 1821 (1981).

7. K. H. J. BUSCHOW AND P. G. VAN ENGEN, *J. Appl. Phys.* **52,** 3537 (1981).
8. N. A. BLUM, K. MOORIANI, T. O. POEHLER, AND F. G. SATKIEWICHZ, *J. Appl. Phys.* **52,** 1808 (1981).
9. N. TSUYA, K. I. ARAI, AND T. OHSAKA, *IEEE Trans. Magn.* **MAG-14,** 941 (1978).
10. M. TAKAHASHI AND M. KOSHIMURA, *Japan J. Appl. Phys.* **16,** 1711 (1977).
11. Y. SHIMADA AND H. KOJIMA, *J. Appl. Phys.* **50,** 1541 (1979).
12. J. A. ABOAF AND E. KLOKHOLM, *J. Magn. Magn. Mater.* **15–18,** 1385 (1980).
13. T. STOBIECKI AND H. HOFFMAN, *J. Phys. (Paris)* **41,** 485–C8 (1980).
14. K. H. J. BUSCHOW AND P. G. VAN ENGEN, *J. Appl. Phys.* **52,** 3557 (1981).
15. C. L. CHIEN AND K. M. UNRUH, *Phys. Rev. B* **25,** 5970 (1982).
16. U. HEROLD AND U. KÖSTER, *Z. Metallkd.* **69,** 326 (1978).
17. U. HEROLD AND U. KÖSTER, "Rapidly Quenched Metals III" (B. Cantor, Ed.), Vol. 1, p. 281, The Metals Society (1978).
18. I. VINCZE, T. KEMENY, AND S. ARAJS, *Phys. Rev. B* **21,** 937 (1980).
19. T. BJURSTRÖM, *Ark. Kemi Mineral. Geol.* **11A,** 5 (1933).
20. R. HASEGAWA, *Phys. Rev. B* **3,** 1631 (1971).
21. R. HASEGAWA AND R. RAY, *J. Appl. Phys.* **49,** 4174 (1978).
22. C. L. CHIEN, D. MUSSER, E. M. GYORGY, R. C. SHERWOOD, H. S. CHEN, F. E. LUBORSKY, AND J. L. WALTER, *Phys. Rev. B* **20,** 283 (1979).
23. R. C. O'HANDLY, L. I. MENDELSOHN, R. HASEGAWA, R. RAY, AND S. KAVESH, *J. Appl. Phys.* **47,** 4660 (1976).